High Temperature Post-Necking Ductility of Ni–W-Cr–Mo Model Alloy for Molten Salt Reactor Application

Ji-Hyun Yoon [a*], Sang-Yeob Lim[a], Jaeseong An[b], Jung-Min Kim[c], Chaewon Kim[a], Daejong Kim[a]
[a]*Korea Atomic Energy Research Institute 111, Daedeok-Daero 989, Yuseong-Gu, Daejeon, Korea*
[b]*Chungnam National University 99, Daehak-ro, Yuseong-Gu, Daejeon, Korea*
[c]*University of Science and Technology 217,Gajeong-ro, Yuseong-Gu, Daejeon, Korea*
[*]*Corresponding author: jhyoon4@kaeri.re.kr*

Keywords **:** Molten Salt Reactor, Structural Materials, Type 316H Stainless Steel, Thermal Spray, Cladding

1. Introduction

Ni-based alloys are leading candidates for molten salt reactor (MSR) structural service because Ni forms a low-solubility passive response in chloride salts when alloyed with sufficient Cr and Mo, while the FCC matrix provides good high-temperature formability and creep resistance [1,2]. Post-necking ductility at operating temperature is a key figure of merit for accident-tolerant behavior and for margin against Te-induced inter-granular attack, a well-known degradation mode in Ni-based alloys exposed to fission-product tellurium [3]. The effects of a modest Cr/Mo increment in an Nb/Hf-modified Ni-based alloy on tensile behavior at 700 °C, using two focal alloys from an in-house seven-alloy development series: NH2 (Ni–10W-8Cr–4Mo) and NH4 (Ni–10W-10Cr–6Mo) was examined in this study. The two alloys share every other alloying element at closely matched content and were processed identically, isolating the effect of Cr/Mo on high-temperature ductility.

2. Experimental

2.1 Materials

NH2 and NH4 alloy compositions measured by ICP-OES and carbon-sulfur combustion analysis are listed in Table 1. Both alloys share a common base composition (W, Fe, Nb, Ti, Hf, Al, Si, Mn closely matched between the two) and differ in Cr, Mo, and carbon content. Ingots were solutionized at 1250°C for 24–48 h, hot-rolled 80% at 1200°C, cold-rolled 10%, and annealed at 930°C for 2 h followed by furnace cooling.

Table 1. Chemistries of model alloys (in wt%) measured by ICP-OES and carbon-sulfur combustion analysis.

Alloy	C	Cr	Mo	W	Fe	Nb	Hf	Ni
NH2	0.028	8.03	4.03	9.88	2.92	1.89	0.20	Bal.
NH4	0.065	10.09	6.00	10.07	2.88	1.91	0.20	Bal.

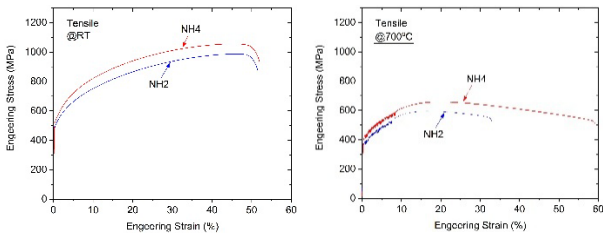
2.2 Tensile testing and characterization

Uniaxial tensile tests were performed at room temperature and 700°C on miniature dog-bone specimens (gage length 12 mm; reduced section 15 × 3 × 1 mm) using a Shimadzu AGS-10kNX STD universal testing machine (10 kN) at a nominal strain rate of 5.6×10^{-4}/s. Two specimens per alloy per temperature were tested. Post-tensile microstructures were characterized by EBSD at two locations of each failed 700 °C specimen: ≈1 mm below the fracture surface (“near-fracture”) and in the region adjacent to the grip (“grip shoulder”, a low-strain reference). Carbide phases were identified by XRD, TEM-SAED on FIB lift-outs, EDS, and CALPHAD (Thermo-Calc).

3. Results and Discussion

3.1 Tensile behavior

Engineering stress–strain curves are shown in Fig. 1. At room temperature (Fig. 1a) NH2 and NH4 exhibit essentially identical total elongations (both 53%) and closely similar UTS (990 vs. 1056 MPa; NH4 +7%). At 700 °C (Fig. 1b) the two alloys reach comparable UTS (604 vs. 665 MPa) and closely similar uniform elongation (18 vs. 20%), but the total elongation diverges dramatically (32 vs. 57%). The post-necking elongation (TE − UE) is 14% for NH2 but 37% for NH4 — a factor of 2.6× higher. Remarkably, NH4’s total elongation is essentially unchanged from RT to 700 °C (53 to 57%), while NH2’s drops substantially (53 to 32%). This temperature-dependent, post-necking-specific divergence rules out an athermal composition-only origin and points to a mechanism activated by thermally driven processes at elevated temperature.



(a) (b)

Fig. 1. Engineering stress–strain curves for NH2 and NH4, cold-rolled. (a) Room temperature: identical total elongations (both 53%). (b) 700 °C: NH4 reaches 57% total elongation vs. 32% for NH2, with the difference concentrated post-necking (37% vs. 14%).

3.2 Grain-boundary evolution

Grip-shoulder EBSD (low-strain reference) shows that NH2 and NH4 begin tensile testing with closely similar, high-angle-boundary (HAGB)-dominated grain-boundary networks (83.3 vs. 85.5% HAGB at the >15°

threshold) and similar Σ3 annealing-twin fractions (Table 2). At the near-fracture location the two alloys diverge sharply: NH2 collapses to 31.8% HAGB (a ≈51.5-percentage-point drop) at only 32% total elongation, whereas NH4 preserves 66.1% HAGB (a ≈19.4-percentage-point drop) despite reaching 57% total elongation. The Σ3 fraction shows the same pattern. That the alloy absorbing nearly twice the plastic strain preserves both HAGB and Σ3 far better than its less-strained counterpart is inconsistent with a simple strain-proportional degradation and indicates a genuine, intrinsic resistance in NH4 to strain-driven conversion of the grain-boundary network into a low-angle, sub-grain-dominated substructure.

Table 2. Grain-boundary character (HAGB, >15°; Σ3) at grip shoulder and near-fracture locations, extracted from EBSD.

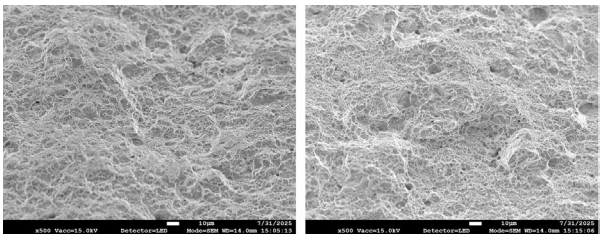
Alloy	Location	HAGB (%)	Σ3 (%)	TE (%)
NH2	Grip shoulder	83.3	58.4	—
NH2	Near-fracture	31.8	20.6	32
NH4	Grip shoulder	85.5	60.9	—
NH4	Near-fracture	66.1	46.4	57

3.3 Precipitate identification

TEM-SAED on FIB lift-outs of NH4 combined with EDS composition matching, composition-constrained XRD lattice-parameter refinement (a ≈ 11.05–11.08 Å), and CALPHAD independently identify a fine population of W-, Mo-, Nb-rich M_6C-type carbides (η-carbide, Fd3m) in NH4, additional to the coarse (Nb,Ti)-rich primary MC carbides shared with NH2. Equilibrium CALPHAD (Thermo-Calc) shows qualitatively different M_6C stability in the two alloys: in NH4 the solvus (≈1000 °C) lies above the 930 °C anneal so M_6C is stable throughout the heat treatment, whereas in NH2 the solvus (≈830 °C) lies below the anneal so M_6C can only re-precipitate during furnace cooling. The equilibrium M_6C volume fraction predicted for NH4 (≈2.4 vol.%) is ≈3× that predicted for NH2 (≈0.8 vol.%). The higher Cr and Mo content of NH4 raises both the M_6C solvus and the thermodynamic driving force; the measured 2.3× higher carbon content of NH4 (0.065 vs. 0.028 wt%; Table I) additionally increases the stoichiometric C supply. Whether NH2 contains any comparable M_6C is under direct investigation.

3.4 Fractography and mechanism

Post-fracture SEM (Fig. 2) shows ductile microvoid coalescence in both alloys, with fine second phase particles at dimple centers. Automated dimple segmentation (≤ 18,000 dimples) gives similar mean dimple size but denser and more uniform dimples in NH4. We attribute NH4's superior high-temperature post-necking ductility to two complementary temperature-activated effects: (i) Mo-induced reduction of matrix stacking-fault energy [4], which restricts cross-slip and delays dynamic recovery of the dislocation substructure; and (ii) Zener-type restraint of boundary reorganization by fine M_6C [5]. Both mechanisms act post-necking and are inactive at RT — explaining why the composition effect emerges only at 700 °C.



(a) (b)

Fig. 2. Post-fracture SEM (×500) of 700°C tensile specimens: (a) NH2 and (b) NH4. Both alloys show ductile micro-void coalescence; NH4 exhibits denser and more uniform dimples.

4. Conclusions

Raising Cr from 8 to 10 wt.% and Mo from 4 to 6 wt.% in an Nb/Hf-bearing Ni-based MSR alloy leaves room-temperature ductility unchanged (TE 53% for both alloys) but raises 700 °C total elongation from 32 to 57% and post-necking elongation from 14 to 37% (2.6×). Grip-shoulder EBSD establishes that the two alloys begin tensile testing with closely similar HAGB-dominated grain-boundary character; the ductility gain therefore arises from a strain-driven, temperature-activated mechanism. Fine M_6C precipitation, forming during furnace cooling and expected to be denser in NH4 owing to both higher Cr/Mo and higher C, provides Zener-type restraint of boundary reorganization complementary to the Mo solid-solution effect. This offers a design pathway to accident-tolerant Ni-based MSR alloys.

REFERENCES

[1] D. F. Williams, L. M. Toth, K. T. Clarno, Assessment of candidate molten salt coolants for the Advanced High-Temperature Reactor (AHTR), ORNL/TM-2006/12, Oak Ridge National Laboratory, 2006.

[2] A. Delagnes et al., A new nickel-based alloy for Molten Salt Reactors using chloride salts, J. Nucl. Mater., 620 (2026) 156353.

[3] H. E. McCoy, Jr., Status of materials development for molten salt reactors, ORNL/TM-5920, Oak Ridge National Laboratory, 1978.

[4] R. E. Schramm, R. P. Reed, Stacking fault energies of seven commercial austenitic stainless steels, Metall. Trans. A 6, 1345–1351 (1975).

[5] C. S. Smith, Grains, phases, and interfaces: an interpretation of microstructure, Trans. AIME 175, 15–51 (1948).